AGU ADVANCING EARTH AND SPACE SCIENCE

Geophysical Research Letters®

RESEARCH LETTER
10.1029/2021GL094719

Key Points:

- The Atlantic Multidecadal Variability cooling can drive an Interdecadal Pacific Oscillation-like warm-phase pattern
- The North Atlantic cooling excites a tropical Gill-type response and midlatitude Rossby wave train responses
- Both the tropical and midlatitude dynamical pathways are central to the decadal-scale trans-basin Atlantic-Pacific connection

Supporting Information:

Supporting Information may be found in the online version of this article.

Correspondence to:

S.-L. Yao and W. Zhou,
yaoshl08@hotmail.com;
wenzhou@cityu.edu.hk

Citation:

Yao, S.-L., Zhou, W., Jin, F.-F., & Zheng, F. (2021). North Atlantic as a trigger for Pacific-wide decadal climate change. *Geophysical Research Letters*, *48*, e2021GL094719. https://doi.org/10.1029/2021GL094719

Received 11 JUN 2021
Accepted 4 SEP 2021

North Atlantic as a Trigger for Pacific-Wide Decadal Climate Change

Shuai-Lei Yao[1,2,3], Wen Zhou[2,4], Fei-Fei Jin[3], and Fei Zheng[5,6]

[1]State Key Laboratory of Numerical Modeling for Atmospheric Sciences and Geophysical Fluid Dynamics, Institute of Atmospheric Physics, Chinese Academy of Sciences, Beijing, China, [2]School of Energy and Environment, Guy Carpenter Asia-Pacific Climate Impact Center, City University of Hong Kong, Hong Kong, China, [3]Department of Atmospheric Sciences, School of Ocean and Earth Science and Technology, University of Hawai'i at Mānoa, Honolulu, HI, USA, [4]Now at Department of Atmospheric and Oceanic Science, Institute of Atmospheric Sciences, Fudan University, Shanghai, China, [5]School of Atmospheric Sciences, Key Laboratory of Tropical Atmosphere-Ocean System, Ministry of Education, Sun Yat-sen University, Zhuhai, China, [6]Now at Southern Marine Science and Engineering Guangdong Laboratory, Zhuhai, China

Abstract The Interdecadal Pacific Oscillation (IPO) features a basin-scale horseshoe-like sea surface temperature (SST) anomaly pattern. Its cold-phase shift around 1999, implicated as a driver for the early-2000s global warming slowdown, has been potentially linked to the Atlantic warming during the positive-phase Atlantic Multidecadal Variability (AMV). However, the key mechanism for the trans-basin Atlantic-Pacific teleconnection remains debatable. Here, we show that an AMV-SST cooling can initiate a pan-Pacific response. The North Atlantic cooling induces westerly wind anomalies over the central-western equatorial Pacific as Kelvin-wave responses and easterly wind anomalies over the far-eastern equatorial Pacific as Rossby-wave responses. Additionally, anomalous lows are generated over the extratropical North and South Pacific through the midlatitude Rossby wave propagation. The tropical and midlatitude teleconnections act together to develop into a warm-phase IPO-like pattern through the wind-induced latent heat. Our results suggest a potential of advancing the predictability of IPO through a skillful simulation of AMV.

Plain Language Summary The Interdecadal Pacific Oscillation (IPO) is the most prominent mode of decadal climate variability over the whole Pacific basin, characterized by a horseshoe-shaped sea surface temperature (SST) anomaly pattern. Its Atlantic counterpart, the Atlantic Multidecadal Variability (AMV) is characterized by a basin-wide SST warming or cooling pattern across the North Atlantic. In recent decades, the Atlantic warming strongly tied to the positive phase of AMV has significantly strengthened the tropical Pacific cooling, contributing to the recent global warming hiatus. Yet, the root cause of the trans-basin Atlantic-Pacific teleconnection on decadal timescales remains unclear. In this study, using the idealized pacemaker simulations with an imposed AMV-SST anomaly pattern in a fully coupled model, we rigorously investigate how an AMV-SST cooling impacts the Pacific-basin decadal-scale climate change. We found that an AMV cooling initiates a tropical Gill-type response and midlatitude Rossby wave trains. The tropical and midlatitude teleconnections work together to form a warm-phase IPO-like SST anomaly pattern. Our results highlight that realistic simulation of the AMV may improve the predictability of the IPO state and predictions of global warming rates.

1. Introduction

The Interdecadal Pacific Oscillation (IPO) (Power et al., 1999), also called the Pacific Decadal Oscillation (Mantua et al., 1997; Zhang et al., 1997), is a pan-Pacific dominant mode of decadal climate variability, characterized by a tripolar pattern with one-sign SST anomalies in the tropical Pacific and opposite-sign SST anomalies in the western-central regions of North and South Pacific. Its Atlantic counterpart, the Atlantic Multidecadal Variability (AMV) (Ruprich-Robert et al., 2017), which is generally referred to as the Atlantic Multidecadal Oscillation (Kushnir, 1994; Schlesinger & Ramankutty, 1994), is manifested as a multidecadal variation of same-sign SST anomalies in the whole North Atlantic (Ting et al., 2009; Trenberth & Shea, 2006). Both the IPO and AMV have experienced several phase shifts over the past century, with profound impacts on regional and global climate. In particular, the warm-phase AMV and cold-phase

IPO occurred with the North American "Dust Bowl" drought of the 1930s (McCabe et al., 2004; Nigam et al., 2011; Seager et al., 2005). Moreover, the cold-phase AMV and warm-phase IPO have been widely invoked as the main driver of the intense prolonged drought of the 1970s–80s over the Sahel region (Thomas & Nigam, 2018; Villamayor & Mohino, 2015; Zhang & Delworth, 2006) and the late-20th-century global rapid warming (Dai et al., 2015; Trenberth & Fasullo, 2013; Wu et al., 2011; Yao et al., 2016). These considerable climatic consequences worldwide highlight the urgent need to understand the dynamical link between the Atlantic and Pacific decadal SST anomalies.

Especially noteworthy is a prominent trans-basin Atlantic-Pacific connection in recent decades. The rapid tropical Atlantic warming associated with the warm-phase AMV has accelerated tropical Pacific easterly winds (England et al., 2014; McGregor et al., 2014) and amplified tropical Pacific decadal cooling (Cai et al., 2019; Kucharski et al., 2011; Li et al., 2016), thus contributing to the early-2000s hiatus (Kosaka & Xie, 2013; Meehl et al., 2011; Yao et al., 2017). This tropical Atlantic-Pacific teleconnection is established through tropical Atlantic warming trend-induced modulation of the Walker circulation (Kucharski et al., 2011; Li et al., 2016; McGregor et al., 2014). Coupled model results also argue that the observed AMV influences the North Pacific decadal SST variability via the Northern Hemisphere storm tracks and positive ocean-air feedbacks over the North Pacific (Zhang & Delworth, 2007). Statistical results of 118-year observations demonstrate that there exists an Atlantic-Pacific connection at low-frequency timescales (Nigam et al., 2020). Although the tropical (Meehl et al., 2020) and extratropical pathways have been proposed to explain the cross-basin Atlantic-Pacific teleconnection, there is still no agreement on the underlying mechanism of how the AMV drives the IPO on decadal timescales without anthropogenic warming signals.

Here, we rigorously investigate the climate impacts of the cold-phase AMV on the whole Pacific basin by using idealized pacemaker experiments, wherein North Atlantic SSTs are nudged toward the time-invariant spatial pattern corresponding to the internal component of the observed AMV SST anomaly (Figure S1). The results reveal that an AMV-SST cooling forces an IPO-like warm-phase SST pattern through a tropical Gill-type atmospheric response and midlatitude atmospheric teleconnections, both of which are key to establishing the decadal-scale trans-basin Atlantic-Pacific connectivity.

The rest of the paper is outlined as follows. The models and experimental setup are described in Section 2. The results are presented in Section 3. Summaries and discussions are provided in Section 4.

2. Models and Experimental Design

2.1. Idealized Pacemaker Experiments

To explore the Pacific decadal-scale climate response to an AMV-SST cooling, we employ idealized AMV pacemaker experiments with the Institute Pierre-Simon Laplace Climate Modeling Center coupled climate model (IPSL-CM6A-LR; Boucher et al., 2020), performed as part of the Decadal Climate Prediction Project (DCPP; Boer et al., 2016). The atmospheric component is at ∼2° horizontal resolution with 79 vertical layers and the oceanic component is at ∼1° resolution with 75 vertical layers.

Following the previous approach (Ting et al., 2009), the radiatively forced SST variability of observed SST (ERSST V4) (Huang et al., 2015) is extracted by applying a signal-to-noise maximizing empirical orthogonal function (EOF) to the annual-mean global SST derived from the CMIP5 multimodel ensemble mean under historical simulations (1870–2005) and representative concentration pathway 8.5 simulations (2006–2013). Similar to an early study (Ruprich-Robert et al., 2017), the internal component of the AMV (called the AMV index for clarity) is obtained as the residual of observed North Atlantic averaged SST (0°–60°N, from the American coast to Africa and Europe). The AMV spatial pattern is obtained by regressing the observed annual-mean SST at each grid point against the AMV index. A zero-phasing Butterworth filter has been applied to the AMV index before the regression. Note that the AMV index is defined as the residual of the radiatively forced component during 1870–2013 and the AMV spatial pattern is obtained by regression covering the period of 1900–2013 during which observation is more reliable.

Table S1 presents the characteristics of the idealized simulations described below. Three sets of experiments are performed. In the full AMV-SST forcing runs, North Atlantic SSTs are separately restored to time-invariant spatial patterns of the cold-phase and warm-phase AMV corresponding to the internally-generated

component of observed AMV anomaly (Figure S1a), hereafter called AMV− and AMV+. These observed AMV anomalies are superimposed onto the model's daily climatology, allowing us to maintain the model's mean state including all the model biases. To suppress potential instability due to artificial SST gradients, 5° buffer zones are defined extending from 60°N to 65°N and 0° to 5°S. In the tropical AMV-SST forcing runs, observed AMV cold and warm SST anomalies are, respectively, imposed only from 0° to 30°N (Figure S1b), called Trop_AMV- and Trop_AMV+, with buffer zones covering from 30°N to 35°N and 0° to 5°S. In the extra-tropical AMV-SST runs, observed AMV cold and warm SST anomalies are, respectively, imposed only from 30°N to 60°N (Figure S1c), called Ex_AMV− and Ex_AMV+, with buffer zones from 60°N to 65°N and 25°N to 30°N. Additionally, the nonlinearity in the effects of the different phases of AMV is discussed by separately comparing AMV− and AMV+ to a simulation wherein North Atlantic SSTs are nudged toward the model's climatology (CTRL). Outside the nudging regions, the rest of the climate system is fully coupled and free to evolve. All radiative forcing agents are held constant at the preindustrial levels. To reduce model drift due to the experimental setup, each simulation is integrated for 10 model years. Fifty ensemble members for the full AMV runs and 25 ensemble members for other runs are generated through perturbation of atmospheric initial conditions. The first year is considered as a spin-up period and all idealized simulation results are based on the ensemble mean of the last 9-year simulation.

2.2. Idealized Atmosphere-Only Experiments

The Community Atmosphere Model version 5.3 (CAM5.3) (Kay et al., 2015) is utilized to identify the direct atmospheric response of the Pacific climate system to an AMV-SST forcing. We use ∼1° horizontal resolution and 31 vertical layers. We conduct three additional pairs of experiments with CAM5.3 (Table S1), including the full AMV cold-phase and warm-phase configurations (−AMV and +AMV), the tropical AMV cold-phase and warm-phase configurations (−Trop_AMV and +Trop_AMV), and the extra-tropical AMV cold-phase and warm-phase configurations (−Ex_AMV and +Ex_AMV). In these experiments, the different AMV SST anomalies are imposed onto the monthly climatological SST and sea ice fraction from the 500-year control run of IPSL-CM6A-LR. All external forcing agents are fixed at their preindustrial values. Each simulation is spun up for 10 years and then ran for another 30 years. We estimate the CAM5.3 response to an AMV cooling by differentiating the AMV warm SST runs from the AMV cold SST runs.

3. Results

3.1. The AMV Teleconnection to Pacific-Wide Decadal Climate Change

Figure 1 illustrates the response to an AMV-SST cooling (AMV− minus AMV+) in IPSL-CM6A-LR. The Pacific basin features a horseshoe-shaped pattern, characterized by warm SST anomalies stretching from the tropical Pacific to the west coasts of North and South America, and by cold SST anomalies in the western-central North and South Pacific. The pan-Pacific SST anomaly bears a close resemblance to the warm-phase IPO-like pattern, albeit with a small patch of cooling in the far-eastern Pacific. The AMV-SST cooling also induces the tropical Indian Ocean cooling, except for weak warming in the southwestern Indian Ocean. Correspondingly, westerly wind anomalies cover the whole tropical Indian Ocean and the western-central equatorial Pacific, and easterly wind anomalies appear over the eastern equatorial Pacific. Meanwhile, there are a pair of anomalous cyclones over the extratropical North and South Pacific.

To better understand the possible origin of the Pacific-wide climate variability, we investigate the respective role of the tropical and extratropical AMV-SST forcing. The tropical AMV cooling successfully captures an IPO-like warm-phase SST pattern (Figure 1b) though SST warming in the equatorial Pacific and the west coast of South America and the associated atmospheric circulation changes are much weaker than those driven by the full AMV cooling (Figure 1a). The SST and cyclone anomalies over the extratropical North Pacific are both enhanced instead (Figure 1b). Conversely, the extratropical AMV cooling fails to simulate a warm-phase IPO-like pattern, but it generates a cyclonic circulation across the extratropical North Pacific (Figure 1c). This is in contrast with previous studies, indicating an active role of the AMV in driving the northern part of the IPO via the North Atlantic-North Pacific teleconnections (Zhang & Delworth, 2007).

On the other hand, assuming linear additivity of the trans-basin interactions, the sum of the model responses to the tropical and extratropical AMV-SST forcings exhibits cyclonic circulations across the extratropical

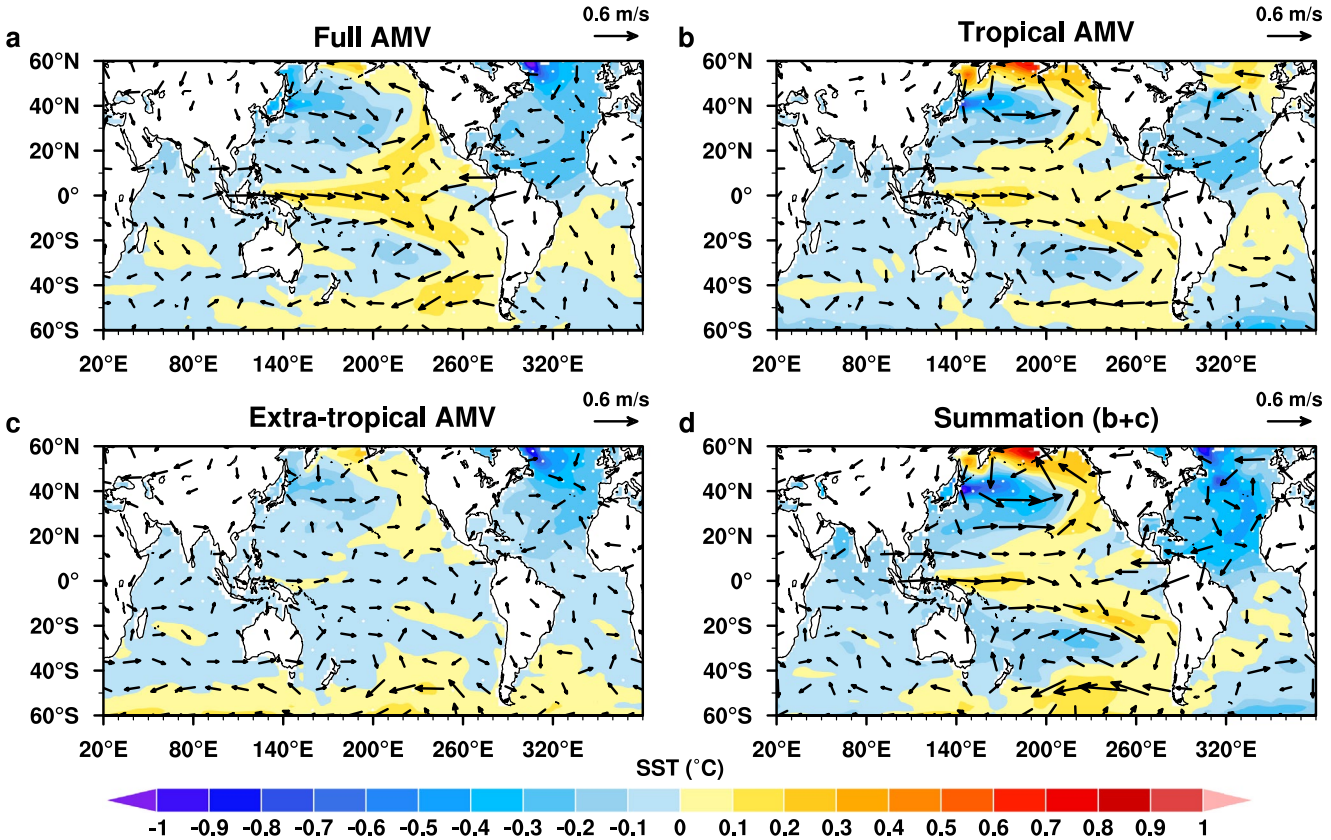

Figure 1. The Atlantic forcing of Pacific-wide decadal-scale climate change in IPSL-CM6A-LR. The last 9-year average difference in sea surface temperature (SST) (shading) and 850-hPa winds (arrows with the key at the top right) from the full Atlantic Multidecadal Variability (AMV) SST forcing (a; AMV− minus AMV+), tropical AMV SST forcing (b; Trop_AMV− minus Trop_AMV+), extra-tropical AMV SST forcing (c; Ex_AMV− minus Ex_AMV+), and a summation (d) of b and c. Stippling indicates regions where more than 67% of members produce the same sign.

Pacific and an IPO-like SST response, but with a larger amplitude compared to the full AMV forcing (cf. Figures 1a and 1d). This discrepancy implies nonlinear interactions between the responses to the tropical and extratropical AMV-SST anomalies. For example, a negative feedback mechanism tends to suppress the response to the tropical AMV-SST anomaly in the presence of the extratropical AMV-SST anomaly and vice versa. This result is different from earlier findings that the tropical AMV-SST forcing acts to amplify the response to the extratropical AMV-SST forcing (Peings & Magnusdottir, 2016; Ruprich-Robert et al., 2017; Sutton & Hodson, 2007). Further work would be required to elucidate the different mechanisms that may be at play in other coupled climate models. Nevertheless, these studies demonstrate that the tropical and extratropical AMV-SST anomalies together drive a significant response of the IPO-like SST pattern in coupled models.

We further examine the Pacific basin-wide response to a warm-phase AMV in IPSL-CM6A-LR (Figure S2). Consistent with earlier findings (Meehl et al., 2020; Ruprich-Robert et al., 2017), the warm-phase AMV SST anomalies (AMV+ minus AMV−) cause an IPO-like cold-phase SST pattern and two anticyclones over the extratropical Pacific. The Pacific-wide climate responses are more sensitive to tropical AMV warm SST effects (Trop_AMV+ minus Trop_AMV−) than extratropical AMV warm SST effects (Ex_AMV+ minus Ex_AMV−). Note, however, that the tropical AMV SST forcing alone is not sufficient to explain the basin-wide IPO-like SST pattern. Therefore, here we mainly focus on the dynamical pathways by which a full AMV-SST cooling excites the Pacific-wide climate changes.

3.2. Tropical Pathway for Relaying the AMV Signal to the Pacific Basin

In the tropics, Atlantic SST cooling (AMV− minus AMV+ in IPSL-CM6A-LR) produces intense rainfall deficits over the north tropical Atlantic (Figure 2a). The associated diabatic cooling excites a typical quadrupole atmospheric response (Figure 2a), with a pair of cyclones occupying the Indian Ocean and the western-central Pacific and a pair of anticyclones extending from the far-eastern Pacific to the tropical Atlantic. The anomalous circulation pattern largely resembles the classic Gill-type response (Gill, 1980), as illustrated by the transient response to an AMV cooling (see more details in Supporting Information S1 and Figure S3). The consequential convection shifts induce a reduced Indo-Pacific Walker circulation (Figure 2b), with anomalous rising motion over the central Pacific and anomalous subsidence over the eastern Indian Ocean. These significant atmospheric responses are well reproduced by the tropical AMV cooling forcing (Figure S4) though some salient features are not reliably captured. Specifically, the tropical AMV cooling-induced cyclonic circulation anomalies are confined mostly to the tropical Pacific (Figure S4a), and the Walker circulation over the Indian Ocean erroneously strengthens (Figure S4b), suggesting the importance of the full AMV cooling in driving the Gill-type response and changes in the Pacific Walker circulation. Note that it is difficult to separate the relative contributions of the Gill-type response and the Walker circulation changes to tropical Pacific surface wind anomalies (Johnson et al., 2020; Y. Takaya et al., 2021).

The Kelvin-wave-generated surface westerly wind anomalies induce a weakened SST gradient over the western-central equatorial Pacific, which in turn amplifies anomalous westerly winds, eventually leading to an El Niño-like state via the Bjerknes feedback (Bjerknes, 1969). In response to anomalous equatorial westerly winds, a warmer subsurface temperature is co-located with anomalous eastward zonal currents (Figure 2c), along with downwelling across the central equatorial Pacific through Ekman pumping. Conversely, the Rossby-wave-induced easterly wind anomalies cool the far-eastern equatorial Pacific due to upwelling there. Accordingly, the El Niño-type warm SST anomalies are mainly restricted to the central equatorial Pacific and cannot develop further to the eastern equatorial Pacific. These mechanisms are analogous to those that activate the central Pacific-type El Niño events by north tropical Atlantic cooling (Ham et al., 2013). It is worth noting that these pronounced ocean dynamical processes along the equatorial Pacific are negligible in the equatorial Indian Ocean, where there is cooling in the upper 300 m but warming at about 100 m depth (Figure 2c). The Indo-Pacific Ocean subsurface temperature changes are essentially replicated by the tropical AMV cooling (Trop_AMV− minus Trop_AMV+), albeit with a reduced magnitude of the subsurface temperature warming anomaly over the central equatorial Pacific (Figure S4c).

3.3. Midlatitude Pathway for the AMV Driving Pacific Decadal Variability

In addition to the tropical atmospheric and oceanic dynamical processes, a cold-phase AMV can modulate the atmospheric circulation across the extratropical North and South Pacific through the propagation of midlatitude Rossby wave trains. The AMV cold-phase SST anomalies induce a convective cooling (Li et al., 2014, 2015) and lower the 200-hPa geopotential height over the tropical Atlantic (AMV− minus AMV+ in IPSL-CM6A-LR; Figure 3a). The negative heating anomaly associated with negative precipitation anomalies emanates stationary Rossby wave trains that first extend to the extratropical North and South Atlantic, then propagate eastward, and ultimately arrive at the midlatitude North and South Pacific (Figure S5). Two active low-pressure centers emerge over the extratropical North and South Pacific, with one in the proximity of the Aleutian Islands and the other to the northeast of New Zealand (Figures 3c and 3e). These two cyclones are nearly equivalently barotropic (Figures 3c and 3e), with a highly similar structure from sea level up to 500 hPa. The low sea level pressure (SLP) patterns over the midlatitude Pacific are broadly comparable with the SLP responses to a tropical AMV cooling forcing (Trop_AMV−- minus Trop_AMV+; Figure S6) though the latter generates an intensified North Pacific cyclone. In contrast, North Pacific low SLP response to the extratropical AMV cooling is comparatively weaker and shifts slightly westward (Ex_AMV− minus Ex_AMV+; Figure S6f).

IPSL-CM6A-LR pacemaker simulations involve atmospheric teleconnections and ocean-air interactions. To single out the direct atmospheric responses to the AMV cooling, three additional sets of atmosphere-only experiments with CAM5.3 are performed, wherein only the observed AMV SST pattern and its tropical and extratropical parts are, respectively, prescribed (Table S1). The atmosphere-only simulations with the full AMV cooling forcing successfully reproduce the Rossby wave train responses (Figure 3b), similar to the full

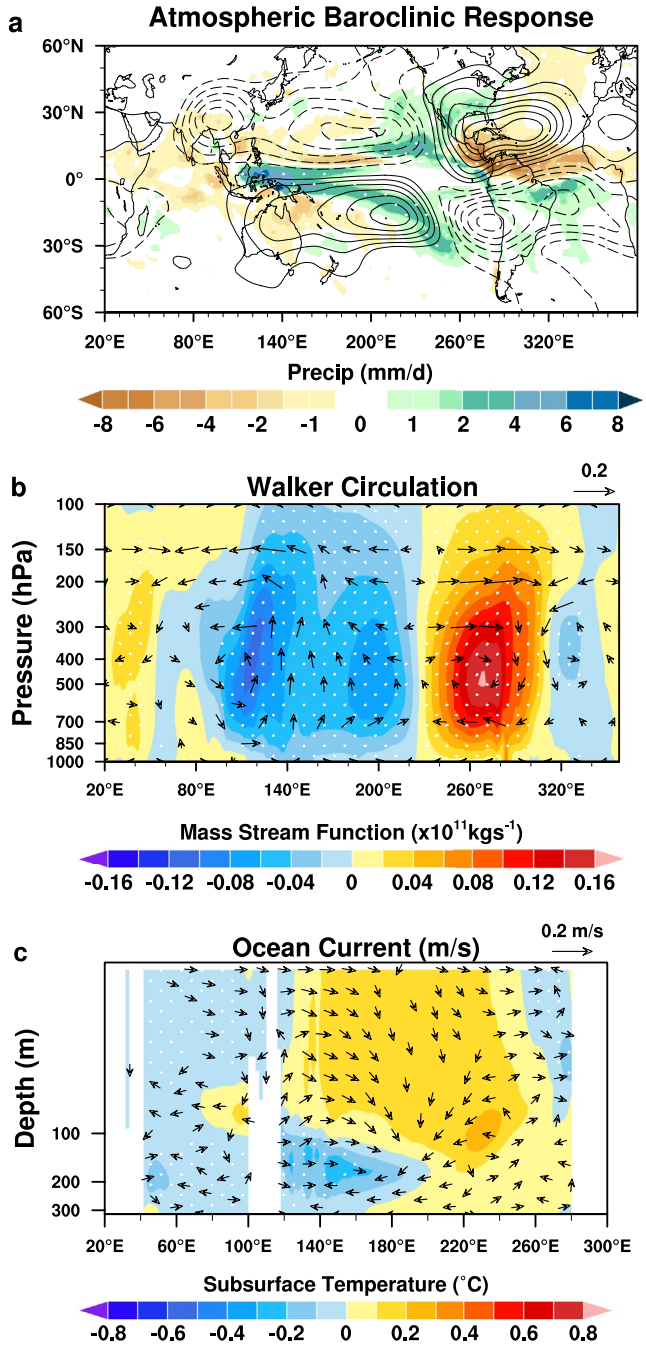

Figure 2. Tropical pathway for an Atlantic Multi-decadal Variability-sea surface temperature cooling driving Pacific decadal climate change in IPSL-CM6A-LR. (a) Precipitation (shading) and atmospheric baroclinic response (contours with interval of 0.2×10^6 kgs^{-1} from -1.2×10^6 kgs^{-1} to 1.2×10^6 kgs^{-1}; solid contours denote positive values). The atmospheric baroclinic response is defined as half the difference between the 850-hPa stream function and the 200-hPa stream function. Note that the zonal mean of the atmospheric baroclinic response has been removed. (b) Zonal mass stream function (shading; overlying arrows represent zonal divergent wind and vertical velocity scaled by a factor of −20). Negative (positive) values show an anti-clockwise (clockwise) rotation and thus a weakened (strengthened) Walker circulation. The zonal mass stream function is estimated by vertically integrating the divergent component of zonal wind meridionally averaged between 6°S and 6°N, from the top-level downward. (c) Equatorial (2°S to 2°N) subsurface temperature (shading) and oceanic zonal currents and vertical velocities (arrows with the key at top right). The results are shown from the last 9-year average difference between the full AMV cold-phase simulations and the full AMV warm-phase simulations (AMV− minus AMV+). Stippling and green lines denote regions where more than 67% of members produce the same sign.

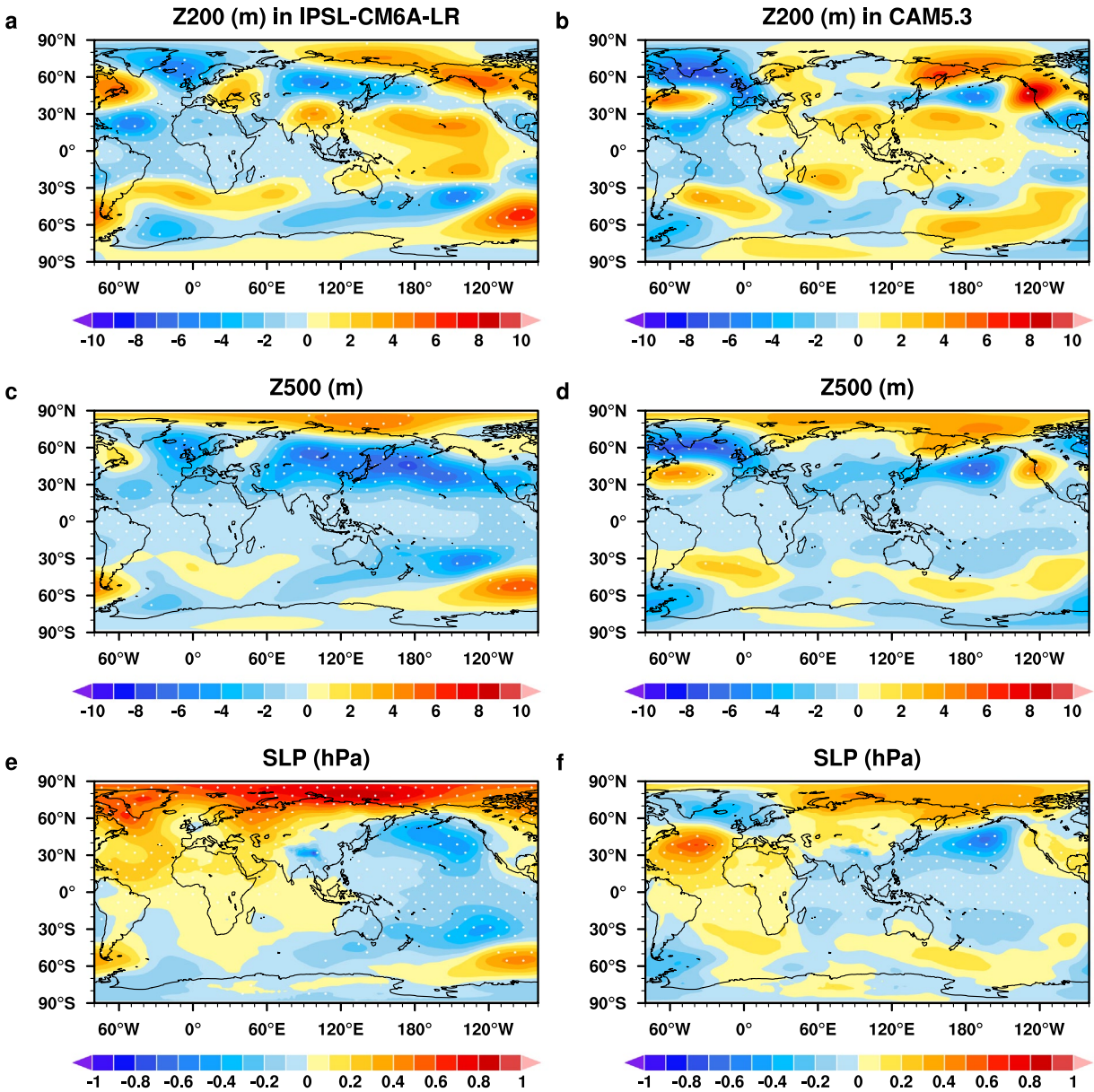

Figure 3. Midlatitude pathway for an Atlantic Multi-decadal Variability-sea surface temperature cooling driving Pacific decadal climate change. The last 9-year average difference in 200-hPa geopotential height with zonal mean removed (a-b; Z200), 500-hPa geopotential height (c–d; Z500), and sea level pressure (e–f; SLP) from the full AMV cold-phase simulations minus the full AMV warm-phase simulations in IPSL-CM6A-LR (left panel: AMV− minus AMV+) and the atmosphere-only simulations with CAM5.3 (right panel: −AMV minus +AMV). Stippling in the left panel is shown where more than 67% of members produce the same sign, and stippling in the right panel is shown above 95% significance based on a two-sided Student's *t* test.

AMV pacemaker simulation results (Figure 3a), albeit with a westward shift. This discrepancy implies that the propagation of midlatitude Rossby wave trains may be sensitive to the location and intensity of the background flow (Fogt et al., 2011; Karoly, 1989; K. Takaya & Nakamura, 2001; Wallace & Gutzler, 1981), such as the subtropical/midlatitude jets (Li et al., 2015). Remarkably, the cyclonic circulation responses over the extratropical Pacific match well with the full AMV pacemaker simulation results (Figures 3d and 3f). The two low SLP anomalies, however, are relatively weaker in the atmosphere-only simulations (Figures 3d and 3f, and S7). Thus, in idealized AMV pacemaker experiments, these two low-pressure centers may be amplified partly by local ocean-air feedback and ocean dynamics (Amaya et al., 2019; Ruprich-Robert et al., 2017) over the midlatitude Pacific, or convective heating anomalies across the equatorial Pacific through the Pacific-North American and Pacific-South American teleconnections (Barsugli & Sardeshmukh, 2002; Trenberth

et al., 2014). The strong coherency between the idealized atmosphere-only and pacemaker simulations reveals the causality and provides support for the existence of the midlatitude dynamical pathways for an AMV cooling to affect the two anomalous cyclones centered in the North and South Pacific.

3.4. Attribution of an IPO-Like Warm-Phase SST Response to an AMV Cooling Based on Ocean Mixed-Layer Heat-Budget Analysis in IPSL-CM6A-LR

To shed new light on how an AMV-SST cooling drives an IPO-like warm SST pattern, we perform a mixed-layer heat-budget analysis (Xie et al., 2010; Yao et al., 2016). The heat-budget equation can be expressed as follows:

$$C\frac{\partial T'}{\partial t} = Q_S + Q_L + Q_H + Q_E + D_o \tag{1}$$

where T' is SST change. The right-hand side includes ocean dynamics (D_o), shortwave radiation (Q_S), longwave radiation (Q_L), and turbulent fluxes of sensible heat (Q_H) and latent heat (Q_E).

For our discussion of SST spatial pattern formation, the ocean dynamics and net surface heat flux are in a quasi-equilibrium. We can rewrite Equation 1 as a diagnostic equation of SST anomaly (see detailed derivation in Supporting Information S1):

$$T' = \frac{Q_S + Q_{L+} + Q_H - Q_{E,W} - Q_{E,\mathrm{RH}} - Q_{E,\Delta T} + D_o}{\alpha\overline{Q_E}} \tag{2}$$

The right-hand side in Equation 2 refers to the SST changes due to variations in shortwave radiation, longwave radiation, sensible heat flux, and changes in latent heat flux caused by variations in near-surface wind speed, relative humidity, or stability, and changes in ocean dynamics, respectively.

We have established that both the tropical Gill-like response and midlatitude Rossby wave trains directly link the North Atlantic to the entire Pacific basin. The large-scale circulation changes in response to the AMV cooling may influence the cross-basin Indo-Pacific SST pattern through changes in surface heat flux. SST changes in the Indo-Pacific basins are in good agreement with the wind-induced latent heat flux (cf. Figures 1a and 4a), which dominates other components of surface heat flux and ocean dynamics (Figures 4b–4g) though they are likely to contribute partly to regional SST anomalies. The Kelvin-wave-induced westerly wind anomalies amplify near-surface wind speed (solid contours in Figure 4a) and enhance evaporation, leading to cooling over the tropical Indian Ocean through the wind-evaporation-SST feedback (Xie et al., 2010). In comparison, the westerly wind anomalies reduce the trade winds, and the wind-related latent heat flux increases, ultimately heating the western-central tropical Pacific. There appear small cooling patches over the far-eastern equatorial Pacific, due mainly to accelerated easterly winds induced by the Gill-type Rossby waves.

Over the North and South Pacific, the two anomalous cyclones in response to the AMV cooling intensify westerly wind anomalies across the subtropical Pacific and thus induce pronounced SST cooling there (Figure 4a). Additionally, these anomalous cyclones slacken near-surface wind speed across the ocean sectors adjacent to North and South America and suppress evaporation, generating SST warming there. The northward and southward advection of warm moist air may also contribute to an SST increase off the west coasts of America.

Does the Pacific basin-wide SST response covary with wind-related latent heat flux? We evaluate the time evolution of the Pacific-wide SST response and wind-induced latent heat flux in the full AMV pacemaker simulations (AMV− minus AMV+) from year 2 to year 10. The Pacific SST response (Figure S8) is a dynamic adjustment to the full AMV cooling through wind-related latent heat flux (Figure S9). To reduce the uncertainty owing to the Pacific mean state, we robustly estimate the IPO-like warm-phase SST response to the AMV cooling by calculating the last 9-year ensemble simulations. Taken together, our results confirm that the wind-related latent heat flux is the main driver of a warm-phase IPO-like SST response.

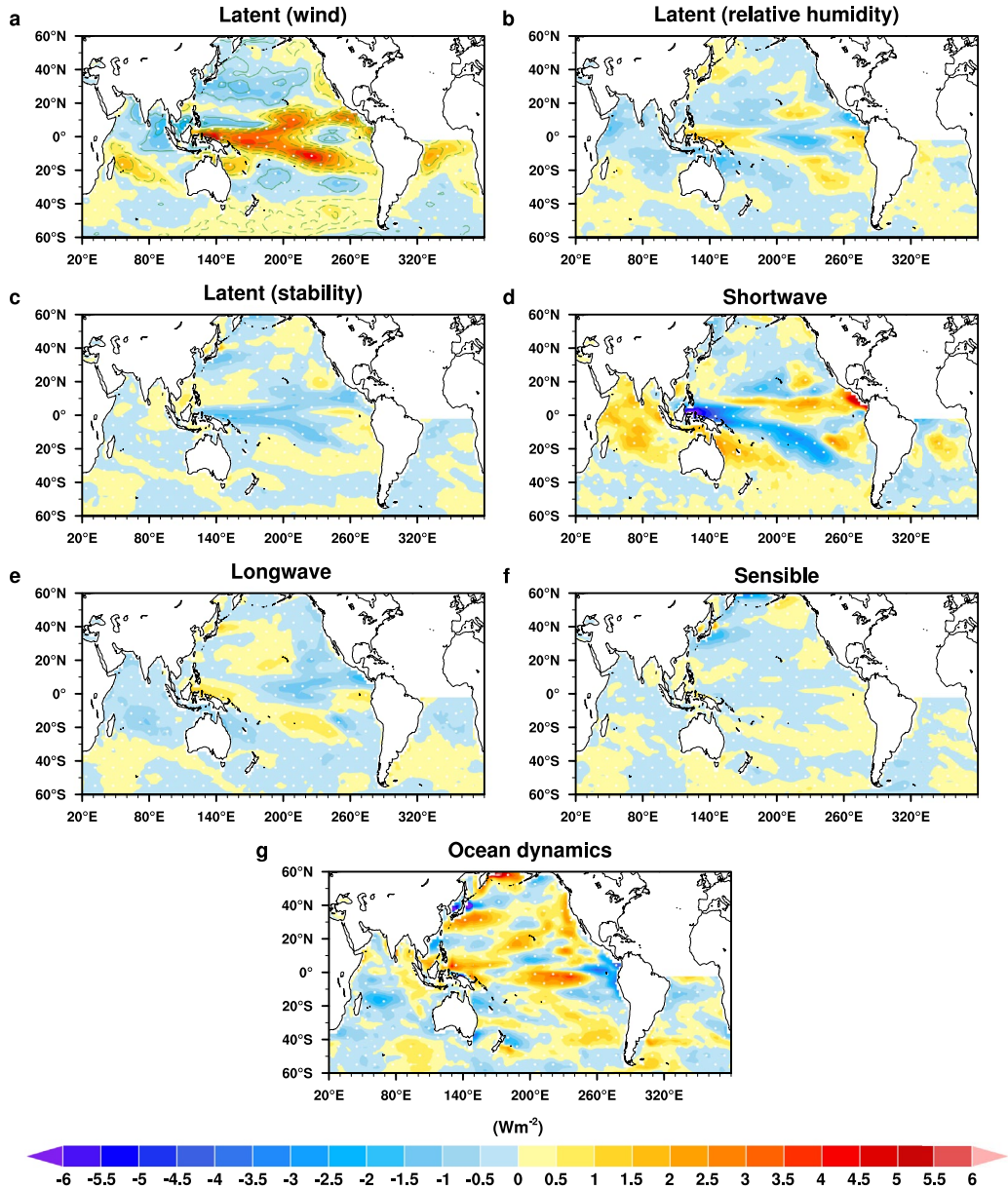

Figure 4. Ocean mixed-layer heat budget analysis in IPSL-CM6A-LR. The last 9-year average difference between AMV− minus AMV+ for (a) latent heat flux due to variations in near-surface wind speed (shading representing wind-induced latent heat and contours with an interval of 0.03 m/s from −0.24 to 0.24 m/s; solid contours mark increased wind speed), (b) latent heat flux due to changes in relative humidity or (c) stability, (d) shortwave radiation, (e) longwave radiation, (f) sensible heat flux, and (g) ocean dynamics. Stippling and green lines indicate regions where more than 67% of members yield the same sign.

4. Summary and Discussion

Our model results demonstrate that an AMV cooling can force a warm-phase IPO-like SST pattern, with tropical Pacific warming extending northeastward and southeastward to both hemispheres and cooling in the western-central parts of the North and South Pacific. The tropical atmospheric response to North Atlantic SST cooling exhibits anomalous westerly winds over the western-central equatorial Pacific through the Gill-type Kelvin-wave responses and anomalous easterly winds in the far-eastern equatorial Pacific because of the Gill-type Rossby-wave responses. The westerly wind anomalies cause the western-central equatorial Pacific warming via the Bjerknes feedback, and this warming is limited to the central equatorial Pacific due

to Ekman pumping there. In contrast, there exists a small cooling area over the far-eastern equatorial Pacific, owing to the local anomalous easterly wind-induced upwelling and the increased latent heat loss from the ocean to the atmosphere. Moreover, the cold-phase AMV produces two active cyclones over the extratropical North and South Pacific through the midlatitude Rossby wave responses. The tropical and midlatitude teleconnections eventually lead to a Pacific-wide horseshoe-like SST pattern through the wind-induced latent heat flux. As a result, both the tropical and midlatitude dynamical pathways from the AMV cooling are of vital importance to the Pacific basin-wide climate change at decadal timescales.

There is an indication of the nonlinearity of the Pacific-wide climate responses to the cold and warm phases of the AMV. We test this hypothesis (Figure S10) by comparing the individual pacemaker experiments (AMV− and AMV+) to the control experiment (CTRL). In the case of the tropical linear response, the impact of a cold-phase AMV (AMV− minus CTRL) is approximately equal but opposite in sign to the impact of a warm-phase AMV (AMV+ minus CTRL). Consistent with a previous study of atmosphere-only simulations (Sutton & Hodson, 2007), tropical Pacific SST and SLP anomalies that project onto the tropical part of an IPO-like pattern are both broadly similar. However, the warm-phase AMV forcing causes larger precipitation anomalies over the intertropical convergence zone than the cold-phase AMV forcing. Contrary to the tropical linearity, the extratropical Pacific responses are highly nonlinear. Particularly noteworthy are the extratropical Pacific strong SLP responses to the warm-phase AMV forcing. Although we assume linearity in the responses to the cold-phase and warm-phase AMV and estimate the difference between the negative AMV-SST anomaly case and the positive AMV-SST anomaly case, our results offer confidence in the robustness of the decadal-scale trans-basin Atlantic-Pacific teleconnection by maximizing the signal-to-noise ratio and investigating the consequence of a shift from a warm-phase to cold-phase AMV.

The magnitude of an IPO-like SST response to an AMV-SST forcing is model-dependent (Meehl et al., 2020; Ruprich-Robert et al., 2017). A recent study assessing 13 coupled model idealized AMV pacemaker simulations points out that the intermodel spread varies by a factor of 10 (Ruprich-Robert et al., 2021), mostly stemming from model precipitation mean-state biases-induced moist static energy injected into the upper troposphere from the Atlantic surface. Earlier studies have also stressed that the Pacific-wide decadal variability is underrepresented in coupled models because of the tropical Atlantic SST mean-state biases (Kajtar et al., 2016; McGregor et al., 2018) or the tropical Pacific mean-state biases (Li et al., 2020). These coupled model mean-state errors limit our ability to better understand the decadal-scale inter-basin Atlantic-Pacific interactions. Given the importance of the decadal-scale trans-basin Atlantic-Pacific connection on climate variability at regional and global scales, decadal climate predictions and future climate projections could be substantially improved if the AMV and IPO states were appropriately initialized in coupled models.

Acknowledgments
This work was supported by the Chinese Postdoctoral Innovative Talent Program (119100582Q), International cooperation and exchange program of National Science Foundation of China (42120104001), and the National Youth Fund Program of China (42005134). S.-L. Yao was supported by the Chinese Scholarship Council. W. Zhou was supported by the Hong Kong RGC General Research Fund (11300920). F. Zheng was supported by the National Natural Science Foundation of China (41775090 and 4179047). We thank the World Climate Research Programme's Working Group on coupled modeling for providing the model datasets. We are grateful to the Institute Pierre-Simon Laplace Climate Modeling Center and the National Center of Atmospheric Research for making IPSL-CM6A-LR model outputs and CAM5.3 available, respectively. We thank Dr. Renguang Wu for his comments that helped us to improve the manuscript. We also thank anonymous reviewers for their constructive comments that contributed to improving the manuscript.

Conflict of Interest

The authors declare no conflicts of interest relevant to this study.

Data Availability Statement

ERSST version 4 is available at https://www.ncdc.noaa.gov/data-access/marineocean-data/extended-reconstructed-sea-surface-temperature-ersst-v4. All idealized pacemaker experiment data are available at https://esgf-node.llnl.gov/search/cmip6/. The CAM5.3 output used in this study is available at https://figshare.com/articles/dataset/CAM5_output/16543617.

References

Amaya, D. J., Kosaka, Y., Zhou, W., Zhang, Y., Xie, S.-P., & Miller, A. J. (2019). The North Pacific pacemaker effect on historical ENSO and its mechanisms. *Journal of Climate*, *32*(22), 7643–7661. https://doi.org/10.1175/JCLI-D-19-0040.1

Barsugli, J. J., & Sardeshmukh, P. D. (2002). Global atmospheric sensitivity to tropical SST anomalies throughout the Indo-Pacific basin. *Journal of Climate*, *15*(23), 3427–3442. https://doi.org/10.1175/1520-0442(2002)015<3427:gastts>2.0.co;2

Bjerknes, J. (1969). Atmospheric teleconnections from the equatorial Pacific. *Monthly Weather Review*, *97*(3), 163–172. https://doi.org/10.1175/1520-0493(1969)097<0163:atftep>2.3.co;2

Boer, G. J., Smith, D. M., Cassou, C., Doblas-Reyes, F., Danabasoglu, G., Kirtman, B., et al. (2016). The Decadal Climate Prediction Project (DCPP) contribution to CMIP6. *Geoscientific Model Development*, *9*(10), 3751–3777. https://doi.org/10.5194/gmd-9-3751-2016

Boucher, O., Servonnat, J., Albright, A. L., Aumont, O., Balkanski, Y., Bastrikov, V., et al. (2020). Presentation and evaluation of the IPSL-CM6A-LR climate model. *Journal of Advances in Modeling Earth Systems*, *12*(7). https://doi.org/10.1029/2019MS002010

Cai, W., Wu, L., Lengaigne, M., Li, T., McGregor, S., Kug, J.-S., et al. (2019). Pantropical climate interactions. *Science*, *363*(6430), eaav4236. https://doi.org/10.1126/science.aav4236

Dai, A., Fyfe, J. C., Xie, S.-P., & Dai, X. (2015). Decadal modulation of global surface temperature by internal climate variability. *Nature Climate Change*, *5*(6), 555–559. https://doi.org/10.1038/nclimate2605

England, M. H., McGregor, S., Spence, P., Meehl, G. A., Timmermann, A., Cai, W., et al. (2014). Recent intensification of wind-driven circulation in the Pacific and the ongoing warming hiatus. *Nature Climate Change*, *4*(3), 222–227. https://doi.org/10.1038/nclimate2106

Fogt, R. L., Bromwich, D. H., & Hines, K. M. (2011). Understanding the SAM influence on the South Pacific ENSO teleconnection. *Climate Dynamics*, *36*(7), 1555–1576. https://doi.org/10.1007/s00382-010-0905-0

Gill, A. E. (1980). Some simple solutions for heat-induced tropical circulation. *Quarterly Journal of the Royal Meteorological Society*, *106*(449), 447–462. https://doi.org/10.1002/qj.49710644905

Ham, Y.-G., Kug, J.-S., & Park, J.-Y. (2013). Two distinct roles of Atlantic SSTs in ENSO variability: North Tropical Atlantic SST and Atlantic Niño. *Geophysical Research Letters*, *40*(15), 4012–4017. https://doi.org/10.1002/grl.50729

Huang, B., Banzon, V. F., Freeman, E., Lawrimore, J., Liu, W., Peterson, T. C., et al. (2015). Extended Reconstructed Sea Surface Temperature Version 4 (ERSST.v4). Part I: Upgrades and intercomparisons. *Journal of Climate*, *28*(3), 911–930. https://doi.org/10.1175/JCLI-D-14-00006.1

Johnson, Z. F., Chikamoto, Y., Wang, S.-Y. S., McPhaden, M. J., & Mochizuki, T. (2020). Pacific decadal oscillation remotely forced by the equatorial Pacific and the Atlantic Oceans. *Climate Dynamics*, *55*(3), 789–811. https://doi.org/10.1007/s00382-020-05295-2

Kajtar, J. B., Santoso, A., McGregor, S., England, M. H., & Baillie, Z. (2016). Model under-representation of decadal Pacific trade wind trends and its link to tropical Atlantic bias. *Climate Dynamics*, *50*(3), 1471–1484. https://doi.org/10.1007/s00382-017-3699-5

Karoly, D. J. (1989). Southern Hemisphere circulation features associated with El Niño-Southern Oscillation events. *Journal of Climate*, *2*(11), 1239–1252. https://doi.org/10.1175/1520-0442(1989)002<1239:shcfaw>2.0.co;2

Kay, J. E., Deser, C., Phillips, A., Mai, A., Hannay, C., Strand, G., et al. (2015). The Community Earth System Model (CESM) large ensemble project: A community resource for studying climate change in the presence of internal climate variability. *Bulletin of the American Meteorological Society*, *96*(8), 1333–1349. https://doi.org/10.1175/BAMS-D-13-00255.1

Kosaka, Y., & Xie, S.-P. (2013). Recent global-warming hiatus tied to equatorial Pacific surface cooling. *Nature*, *501*(7467), 403–407. https://doi.org/10.1038/nature12534

Kucharski, F., Kang, I.-S., Farneti, R., & Feudale, L. (2011). Tropical Pacific response to 20th century Atlantic warming. *Geophysical Research Letters*, *38*(3). https://doi.org/10.1029/2010GL046248

Kushnir, Y. (1994). Interdecadal variations in North Atlantic Sea Surface temperature and associated atmospheric conditions. *Journal of Climate*, *7*(1), 141–157. https://doi.org/10.1175/1520-0442(1994)007<0141:ivinas>2.0.co;2

Li, C., Dommenget, D., & McGregor, S. (2020). Trans-basin Atlantic-Pacific connections further weakened by common model Pacific mean SST biases. *Nature Communications*, *11*(1), 5677. https://doi.org/10.1038/s41467-020-19338-z

Li, X., Holland, D. M., Gerber, E. P., & Yoo, C. (2014). Impacts of the north and tropical Atlantic Ocean on the Antarctic Peninsula and sea ice. *Nature*, *505*(7484), 538–542. https://doi.org/10.1038/nature12945

Li, X., Holland, D. M., Gerber, E. P., & Yoo, C. (2015). Rossby waves mediate impacts of tropical oceans on West Antarctic atmospheric circulation in Austral winter. *Journal of Climate*, *28*(20), 8151–8164. https://doi.org/10.1175/JCLI-D-15-0113.1

Li, X., Xie, S.-P., Gille, S. T., & Yoo, C. (2016). Atlantic-induced pan-tropical climate change over the past three decades. *Nature Climate Change*, *6*(3), 275–279. https://doi.org/10.1038/nclimate2840

Mantua, N. J., Hare, S. R., Zhang, Y., Wallace, J. M., & Francis, R. C. (1997). A pacific interdecadal climate oscillation with impacts on Salmon production*. *Bulletin of the American Meteorological Society*, *78*(6), 1069–1080. https://doi.org/10.1175/1520-0477(1997)078<1069:apicow>2.0.co;2

McCabe, G. J., Palecki, M. A., & Betancourt, J. L. (2004). Pacific and Atlantic Ocean influences on multidecadal drought frequency in the United States. *Proceedings of the National Academy of Sciences*, *101*(12), 4136–4141. https://doi.org/10.1073/pnas.0306738101

McGregor, S., Stuecker, M. F., Kajtar, J. B., England, M. H., & Collins, M. (2018). Model tropical Atlantic biases underpin diminished Pacific decadal variability. *Nature Climate Change*, *8*(6), 493–498. https://doi.org/10.1038/s41558-018-0163-4

McGregor, S., Timmermann, A., Stuecker, M. F., England, M. H., Merrifield, M., Jin, F.-F., & Chikamoto, Y. (2014). Recent Walker circulation strengthening and Pacific cooling amplified by Atlantic warming. *Nature Climate Change*, *4*(10), 888–892. https://doi.org/10.1038/nclimate2330

Meehl, G. A., Arblaster, J. M., Fasullo, J. T., Hu, A., & Trenberth, K. E. (2011). Model-based evidence of deep-ocean heat uptake during surface-temperature hiatus periods. *Nature Climate Change*, *1*(7), 360–364. https://doi.org/10.1038/nclimate1229

Meehl, G. A., Hu, A., Castruccio, F., England, M. H., Bates, S. C., Danabasoglu, G., et al. (2020). Atlantic and Pacific tropics connected by mutually interactive decadal-timescale processes. *Nature Geoscience*, *14*, 36–42. https://doi.org/10.1038/s41561-020-00669-x

Nigam, S., Guan, B., & Ruiz-Barradas, A. (2011). Key role of the Atlantic Multidecadal Oscillation in 20th century drought and wet periods over the Great Plains. *Geophysical Research Letters*, *38*(16). https://doi.org/10.1029/2011GL048650

Nigam, S., Sengupta, A., & Ruiz-Barradas, A. (2020). Atlantic–Pacific Links in observed multidecadal SST variability: Is the Atlantic multidecadal oscillation's phase reversal orchestrated by the Pacific decadal oscillation? *Journal of Climate*, *33*(13), 5479–5505. https://doi.org/10.1175/JCLI-D-19-0880.1

Peings, Y., & Magnusdottir, G. (2016). Wintertime atmospheric response to Atlantic multidecadal variability: Effect of stratospheric representation and ocean–atmosphere coupling. *Climate Dynamics*, *47*(3), 1029–1047. https://doi.org/10.1007/s00382-015-2887-4

Power, S., Casey, T., Folland, C., Colman, A., & Mehta, V. (1999). Inter-decadal modulation of the impact of ENSO on Australia. *Climate Dynamics*, *15*(5), 319–324. https://doi.org/10.1007/s003820050284

Ruprich-Robert, Y., Moreno-Chamarro, E., Levine, X., Bellucci, A., Cassou, C., Castruccio, F., et al. (2021). Impacts of Atlantic multidecadal variability on the tropical Pacific: A multi-model study. *Npj Climate and Atmospheric Science*, *4*(1), 1–11. https://doi.org/10.1038/s41612-021-00188-5

Ruprich-Robert, Y., Msadek, R., Castruccio, F., Yeager, S., Delworth, T., & Danabasoglu, G. (2017). Assessing the climate impacts of the observed atlantic multidecadal variability using the GFDL CM2.1 and NCAR CESM1 global coupled models. *Journal of Climate*, *30*(8), 2785–2810. https://doi.org/10.1175/JCLI-D-16-0127.1

Schlesinger, M. E., & Ramankutty, N. (1994). An oscillation in the global climate system of period 65–70 years. *Nature*, *367*(6465), 723–726. https://doi.org/10.1038/367723a0

Seager, R., Kushnir, Y., Herweijer, C., Naik, N., & Velez, J. (2005). Modeling of tropical forcing of persistent droughts and pluvials over Western North America: 1856–2000. *Journal of Climate*, *18*(19), 4065–4088. https://doi.org/10.1175/JCLI3522.1

Sutton, R. T., & Hodson, D. L. R. (2007). Climate response to basin-scale warming and cooling of the North Atlantic Ocean. *Journal of Climate*, *20*(5), 891–907. https://doi.org/10.1175/JCLI4038.1

Takaya, K., & Nakamura, H. (2001). A formulation of a phase-independent wave-activity flux for stationary and migratory quasigeostrophic eddies on a zonally varying basic flow. *Journal of the Atmospheric Sciences*, *58*(6), 608–627. https://doi.org/10.1175/1520-0469(2001)058<0608:afoapi>2.0.co;2

Takaya, Y., Saito, N., Ishikawa, I., & Maeda, S. (2021). Two tropical routes for the remote influence of the Northern Tropical Atlantic on the Indo–Western Pacific summer climate. *Journal of Climate*, *34*(5), 1619–1634. https://doi.org/10.1175/JCLI-D-20-0503.1

Thomas, N., & Nigam, S. (2018). Twentieth-century climate change over Africa: Seasonal hydroclimate trends and Sahara Desert expansion. *Journal of Climate*, *31*(9), 3349–3370. https://doi.org/10.1175/JCLI-D-17-0187.1

Ting, M., Kushnir, Y., Seager, R., & Li, C. (2009). Forced and internal twentieth-century SST trends in the North Atlantic. *Journal of Climate*, *22*(6), 1469–1481. https://doi.org/10.1175/2008JCLI2561.1

Trenberth, K. E., & Fasullo, J. T. (2013). An apparent hiatus in global warming? *Earth's Future*, *1*(1), 19–32. https://doi.org/10.1002/2013EF000165

Trenberth, K. E., Fasullo, J. T., Branstator, G., & Phillips, A. S. (2014). Seasonal aspects of the recent pause in surface warming. *Nature Climate Change*, *4*(10), 911–916. https://doi.org/10.1038/nclimate2341

Trenberth, K. E., & Shea, D. J. (2006). Atlantic hurricanes and natural variability in 2005. *Geophysical Research Letters*, *33*(12). https://doi.org/10.1029/2006GL026894

Villamayor, J., & Mohino, E. (2015). Robust Sahel drought due to the Interdecadal Pacific Oscillation in CMIP5 simulations. *Geophysical Research Letters*, *42*(4), 1214–1222. https://doi.org/10.1002/2014GL062473

Wallace, J. M., & Gutzler, D. S. (1981). Teleconnections in the Geopotential Height Field during the Northern Hemisphere Winter. *Monthly Weather Review*, *109*(4), 784–812. https://doi.org/10.1175/1520-0493(1981)109<0784:titghf>2.0.co;2

Wu, Z., Huang, N. E., Wallace, J. M., Smoliak, B. V., & Chen, X. (2011). On the time-varying trend in global-mean surface temperature. *Climate Dynamics*, *37*(3), 759. https://doi.org/10.1007/s00382-011-1128-8

Xie, S.-P., Deser, C., Vecchi, G. A., Ma, J., Teng, H., & Wittenberg, A. T. (2010). Global warming pattern formation: Sea surface temperature and rainfall*. *Journal of Climate*, *23*(4), 966–986. https://doi.org/10.1175/2009JCLI3329.1

Yao, S.-L., Huang, G., Wu, R.-G., & Qu, X. (2016). The global warming hiatus—A natural product of interactions of a secular warming trend and a multi-decadal oscillation. *Theoretical and Applied Climatology*, *123*(1), 349–360. https://doi.org/10.1007/s00704-014-1358-x

Yao, S.-L., Luo, J.-J., Huang, G., & Wang, P. (2017). Distinct global warming rates tied to multiple ocean surface temperature changes. *Nature Climate Change*, *7*(7), 486–491. https://doi.org/10.1038/nclimate3304

Zhang, R., & Delworth, T. L. (2006). Impact of Atlantic multidecadal oscillations on India/Sahel rainfall and Atlantic hurricanes. *Geophysical Research Letters*, *33*(17). https://doi.org/10.1029/2006GL026267

Zhang, R., & Delworth, T. L. (2007). Impact of the Atlantic multidecadal oscillation on North Pacific climate variability. *Geophysical Research Letters*, *34*(23). https://doi.org/10.1029/2007GL031601

Zhang, Y., Wallace, J. M., & Battisti, D. S. (1997). ENSO-like interdecadal variability: 1900–93. *Journal of Climate*, *10*(5), 1004–1020. https://doi.org/10.1175/1520-0442(1997)010<1004:eliv>2.0.co;2